THE JOURNAL OF BIOLOGICAL CHEMISTRY
Vol. 250, No. 16, Issue of August 25, pp. 6368-6380, 1975
Printed in U.S.A.

Studies of Individual Carbon Sites of Proteins in Solution by Natural Abundance Carbon 13 Nuclear Magnetic Resonance Spectroscopy

RELAXATION BEHAVIOR*

(Received for publication, December 26, 1974)

ERIC OLDFIELD,‡ RAYMOND S. NORTON, AND ADAM ALLERHAND
From the Department of Chemistry, Indiana University, Bloomington, Indiana 47401

The aromatic regions in proton-decoupled natural abundance ^{13}C Fourier transform nuclear magnetic resonance spectra (at 14.2 kG) of small native proteins contain broad methine carbon bands and narrow nonprotonated carbon resonances. Some factors that affect the use of natural abundance ^{13}C Fourier transform NMR spectroscopy for monitoring individual nonprotonated aromatic carbon sites of native proteins in solution are discussed. The effect of protein size is evaluated by comparing the ^{13}C NMR spectra of horse heart ferrocytochrome *c*, hen egg white lysozyme, horse carbon monoxide myoglobin, and human adult carbon monoxide hemoglobin. Numerous single carbon resonances are observed in the aromatic regions of ^{13}C NMR spectra of cytochrome *c*, lysozyme, and myoglobin. The much larger hemoglobin yields few resolved individual carbon resonances. Theoretical and some experimental values are presented for the natural linewidths (W), spin-lattice relaxation times (T_1), and nuclear Overhauser enhancements (NOE) of nonprotonated aromatic carbons and C^{ζ} of arginine residues. In general, the ^{13}C-^{1}H dipolar mechanism dominates the relaxation of these carbons. ^{13}C-^{14}N dipolar relaxation contributes significantly to $1/T_1$ of $C^{\epsilon 2}$ of tryptophan residues and C^{ζ} of arginine residues of proteins in D_2O. The NOE of each nonprotonated aromatic carbon is within experimental error of the calculated value of about 1.2. As a result, integrated intensities can be used for making a carbon count. Theoretical results are presented for the effect of internal rotation on W, T_1, and the NOE. A comparison with the experimental T_1 and NOE values indicates that if there is internal rotation of aromatic amino acid side chains, it is not fast relative to the over-all rotational motion of the protein.

Nuclear magnetic resonance spectroscopy can be used to monitor individual atomic sites of proteins in solution. Nuclei with non-zero spin that are present in all proteins and are suitable for this purpose (in principle at least) are: ^{1}H, ^{2}H, ^{13}C, ^{14}N, ^{15}N, and ^{17}O. However, practical difficulties of resolution and sensitivity have prevented the general use of most of these nuclei. The ^{1}H nucleus has been the most widely used one for NMR studies of proteins (1-4). In recent years, a number of investigators have turned their attention to ^{13}C NMR of proteins (5-32). Some reports have covered general features in the natural abundance ^{13}C NMR spectra of aqueous proteins in various states (5-11). Others have dealt with ^{13}C NMR signals of incorporated ^{13}C-enriched amino acid residues (12-14) and adducts (15-26). We have chosen to concentrate our efforts on the observation of single carbon resonances in the aromatic regions of the natural abundance ^{13}C NMR spectra of native proteins (27-31). The development of a 20-mm NMR probe has facilitated the detection of these resonances (30). We reserve the term "single carbon resonance" for a signal that arises from just 1 carbon of a monomeric protein. We use the term "individual carbon resonance" to denote a signal that is either a single carbon resonance or the sum of single carbon resonances of two or more equivalent subunits. The term "individual carbon resonance" has been used by some authors to denote a signal that arises from a class of carbon atoms, such as the single peak that results from C^{γ} of all of the threonine residues of calf skin gelatin (9).

We have recently observed numerous single carbon resonances in the aromatic regions of the natural abundance ^{13}C NMR spectra of hen egg white lysozyme (27, 29, 31), horse heart ferrocytochrome *c* (28), horse heart ferricytochrome *c* (28), and horse heart cyanoferricytochrome *c* (31). Opella *et al.* (32) have reported some single carbon resonances in the natural abundance ^{13}C NMR spectrum of carp parvalbumin. Here we present theoretical and experimental results relating to the following questions. Which types of carbons are the most likely to yield resolved single carbon resonances? As the size of

* This work was supported by the National Science Foundation (Grant GP-40688X), the United States Public Health Service (Grant NS-10977-02), and by Eli Lilly and Company.
‡ Supported by a Fellowship from the European Molecular Biology Organization.

the protein molecule increases, how rapidly does the number of resolved single carbon resonances diminish? What type of information can be extracted from measurements of spin-lattice relaxation times (T_1) of individual carbon resonances? Does each carbon yield a resonance of the same intensity, or does one have to take into account differing values of the nuclear Overhauser enhancement? Is it possible to readily count the number of resolved single carbon resonances?

EXPERIMENTAL PROCEDURE

Preparation of samples is described in the following paper (33). ^{13}C NMR spectra were obtained at 15.18 MHz by means of the Fourier transform method. The apparatus has been described (27, 30). The 90° radiofrequency pulses were used for ^{13}C excitation when recording normal Fourier transform NMR spectra. When recording PRFT[1] spectra (34), the nuclear spin magnetization was first inverted by means of a 180° radiofrequency pulse, and then, after an interval τ, 90° radiofrequency pulse excitation was applied. Details have been given (35). For the fully proton-decoupled spectra, the ^1H irradiation (about 0.6 G peak field strength at 60.37 MHz) was centered 6 ppm downfield from the ^1H resonance of Me_4Si, and had a random noise modulation bandwidth of about 10 ppm. For the noise-modulated off-resonance proton-decoupling experiments (27, 36), the ^1H irradiation was centered 8 to 10 ppm upfield from Me_4Si and had a noise modulation bandwidth of about 5 ppm. A spectrum without proton decoupling was recorded by setting the proton irradiation 50 kHz off-resonance and switching off the noise modulation.

Time domain data were accumulated in 8,192 or 16,384 addresses of a Nicolet-1085 computer. Spectral widths of 4,000 Hz or 3,787.9 Hz were used. Fourier transformation was done on 16,384 time domain points in all cases. When only 8,192 addresses were used for data accumulation, 8,192 addresses with a zero value were placed at the end of each block of accumulated time domain data points. In this way, after Fourier transformation there was one point every 0.488 Hz (4,000-Hz spectra) or every 0.462 Hz (3,787.9-Hz spectra). T_1 values were obtained from PRFT spectra (35). Chemical shifts, linewidths, and integrated intensities were measured digitally. Integrated intensities were obtained from spectra that were recorded using a recycle time at least 2.5 times the value of the longest pertinent T_1 value, except for the resonances of C^ζ of arginine residues of hen egg white lysozyme in D_2O.

GENERAL CONSIDERATIONS

Proton-decoupled natural abundance ^{13}C NMR spectra of the diamagnetic proteins horse heart ferrocytochrome *c*, horse carbon monoxide myoglobin, and human adult carbon monoxide hemoglobin are shown in Fig. 1. Each spectrum is divided (27, 33) into the region of carbonyl resonances (about 170 to 210 ppm downfield from Me_4Si), the region of aromatic carbons (about 100 to 160 ppm downfield from Me_4Si), and the region of aliphatic carbons (about 10 to 75 ppm downfield from Me_4Si). The aromatic region also contains C^ζ resonances of arginine residues (33) and vinyl carbon resonances (if present). In each spectrum there are broad features and narrow resonances. Even for the smallest proteins in their native conformation, we expect broad resonances (linewidth $\gtrsim$20 Hz) for α carbons and for protonated side chain carbons not undergoing fast internal rotation (29). Only two types of carbons of a native protein can yield narrow resonances (linewidth $\lesssim$5 Hz): protonated carbons undergoing fast internal rotation, and nonprotonated carbons (29).

The aliphatic carbon region in each spectrum of Fig. 1 contains broad bands and narrow resonances. Since only protonated carbons contribute here, the narrow resonances must arise from aliphatic side chain carbons undergoing fast internal rotation relative to the rate of over-all molecular

[1]The abbreviations used are: PRFT, partially relaxed Fourier transform; NFT, normal Fourier transform; NOE, nuclear Overhauser enhancement.

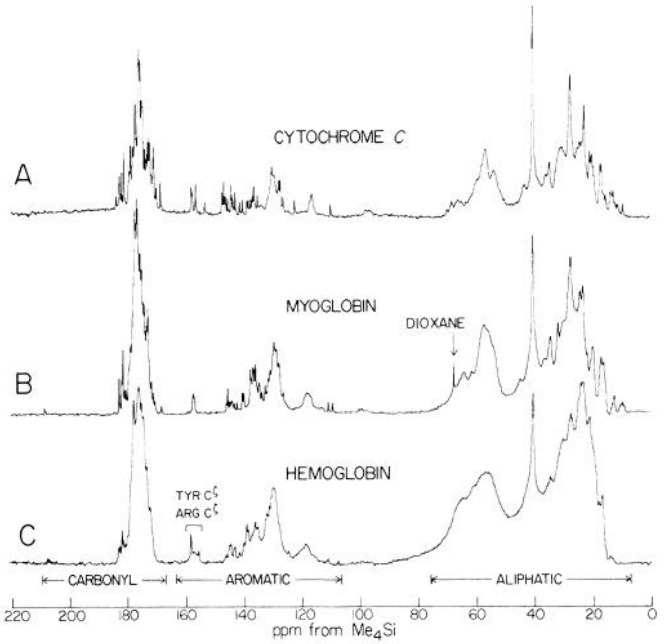

FIG. 1. Fully proton-decoupled natural abundance ^{13}C Fourier transform NMR spectra of some diamagnetic heme proteins in H_2O (0.1 M NaCl/0.05 M phosphate buffer). Each spectrum was recorded at 15.18 MHz using 8,192 time domain addresses, a 4,000-Hz spectral width, 1.105-s recycle time, and 0.62-Hz digital broadening. *A*, 11.5 mM horse heart ferrocytochrome *c*, pH 6.7, 40°, after 16,384 accumulations (5 hours total time). *B*, 9.7 mM horse carbon monoxide myoglobin (plus dioxane), pH 6.7, 36°, after 32,768 accumulations (10 hours total time). *C*, 3.3 mM (in tetramer) human adult carbon monoxide hemoglobin, pH 7.0, 34°, after 32,768 accumulations.

tumbling (10). At 15.18 MHz, we do not expect to find a significant number of resolved single carbon resonances in the saturated carbon region of the natural abundance ^{13}C NMR spectrum of a protein, for two reasons. First, a relatively large number of carbons contribute here. Second, chemical shift nonequivalence caused by folding of the protein into its native conformation is probably diminished as a result of internal rotations. Although we do not discount the possibility of observing single carbon resonances of some saturated side chains, we have concentrated our efforts on nonprotonated carbons.

There are three types of nonprotonated carbons in a protein: carbonyls, C^ζ of arginine residues, and some of the aromatic carbons. Most carbonyls are squeezed into a range of only about 15 ppm (Fig. 1) and yield few resolved single carbon resonances (33, 37). The resonances of C^ζ of arginine residues usually appear at the downfield edge of the aromatic region (33). The relatively small number of aromatic carbons of a protein covers a large range of chemical shifts. Furthermore, protonated (methine) aromatic carbons of native proteins generally give rise to broad resonances, and only nonprotonated aromatic carbons give rise to narrow ones (27–29). In Fig. 2 we show the aromatic regions of the spectra of Fig. 1. Note the presence of broad features and narrow resonances. Some of the narrow peaks are located on top or on the sides of the broad features.

There are seven types of nonprotonated aromatic carbons of amino acid residues: C^γ of phenylalanine, C^γ and C^ζ of tyrosine, C^γ of histidine, and C^γ, $C^{\delta 2}$, and $C^{\epsilon 2}$ of tryptophan residues (Fig. 3). A heme protein also has the 16 nonprotonated aromatic carbons of each heme, which yield narrow resonances in spectra of diamagnetic states of the protein (28, 33, 37). A

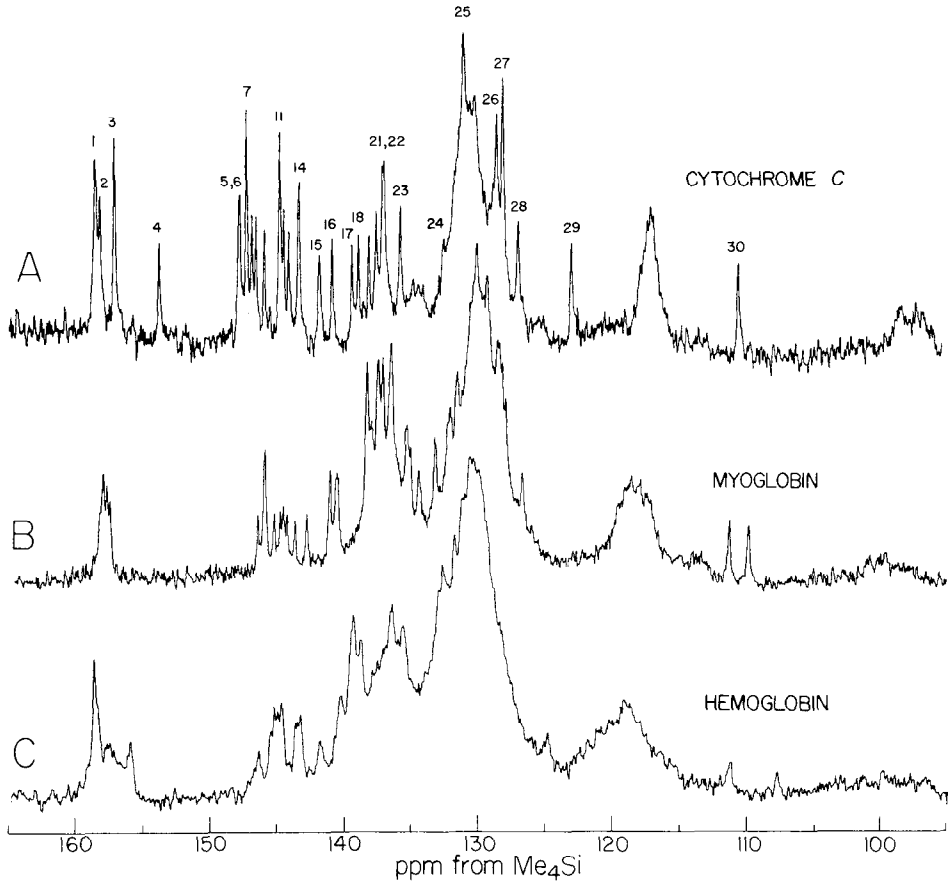

FIG. 2. Region of aromatic carbons and C^{ζ} of arginine residues in fully proton-decoupled natural abundance ^{13}C Fourier transform NMR spectra of some diamagnetic heme proteins. *A*, horse heart ferrocytochrome *c*, from Fig. 1*A*. Peak numbers are those of Refs. 28 and 33. *B*, horse carbon monoxide myoglobin, from Fig. 1*B*. *C*, human adult carbon monoxide hemoglobin, as in Fig. 1*C*, but processed with 0.93-Hz digital broadening.

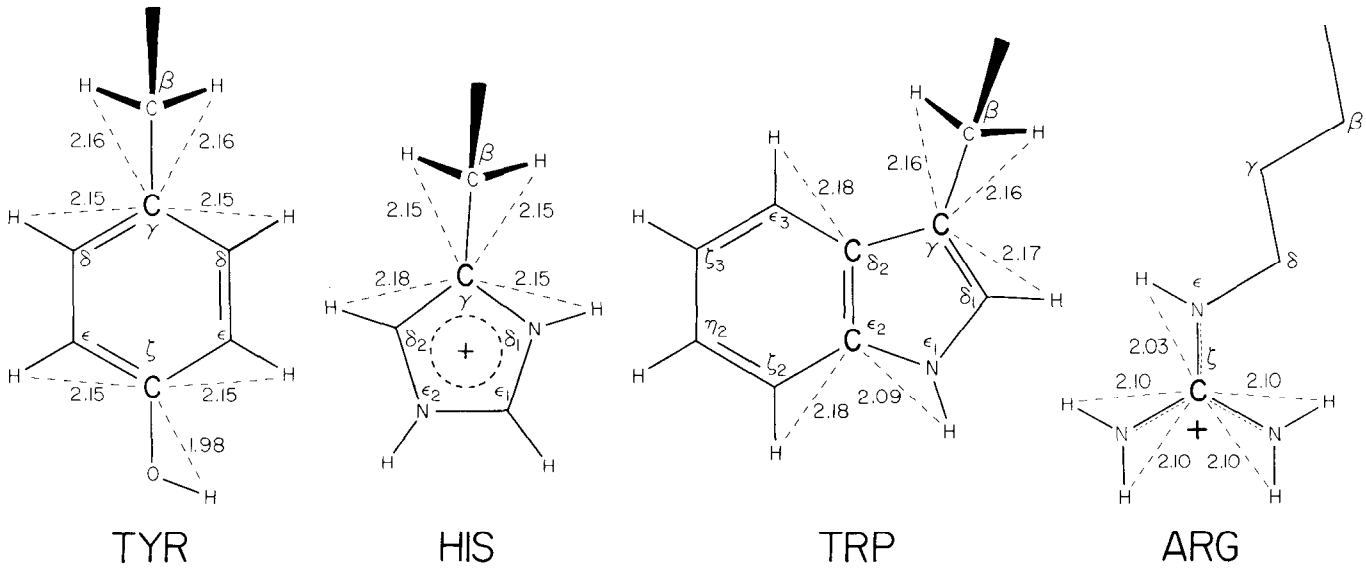

FIG. 3. Estimated distances of nonprotonated side chain carbons (of tyrosine, histidine, tryptophan, and arginine residues) to hydrogens two bonds removed. These distances were computed with the use of known bond lengths and angles (not involving hydrogen) in some crystalline amino acids and small peptides, and known CH, OH, and NH bond lengths in smaller molecules (39, 40). The calculated two-bond CH distances for C^{γ} of phenylalanine are about the same as those shown for tyrosine.

summary of the chemical shift ranges observed for the various types of nonprotonated aromatic carbons of proteins is given in the following paper (33).

Horse heart cytochrome *c* has 34 nonprotonated aromatic carbons, 16 from the heme and 18 from the 4 phenylalanine, 4 tyrosine, 3 histidine, and 1 tryptophan residues (38). If we include C^{ζ} resonances of the 2 arginine residues (Fig. 3), we expect up to 36 narrow single carbon resonances in the aromatic region of the ^{13}C NMR spectrum of horse heart ferrocytochrome *c*. Even at our low magnetic field strength of 14.2 kG, we have observed 20 single carbon resonances and 8 two-carbon resonances (Fig. 2*A*). Some specific assignments are given in the following paper (33). The horse myoglobin molecule contains 44 nonprotonated aromatic carbons, 16 from the heme and the rest from the 7 phenylalanine, 2 tyrosine, 11 histidine, and 2 tryptophan residues (38). We must also

consider C^{ζ} of the 2 arginine residues (38). There is a slight decrease in the number of resolved single carbon resonances when going from horse heart ferrocytochrome *c* (Fig. 2*A*) to horse carbon monoxide myoglobin (Fig. 2*B*). Human adult hemoglobin has 87 nonequivalent nonprotonated aromatic carbons, 32 from the hemes of α and β subunits and 55 from amino acid residues (38). We must also consider C^{ζ} of the 6 nonequivalent arginine residues (38). Not only does hemoglobin contain more than twice the number of nonprotonated aromatic carbons of cytochrome *c*, but the individual carbon resonances of hemoglobin are about twice as broad as those of cytochrome *c* (see below). Predictably, the number of identifiable individual carbon resonances in the ^{13}C NMR spectrum of carbon monoxide hemoglobin (Fig. 2*C*) is small at 15.18 MHz. We present our observations of some resolved individual carbon resonances in the ^{13}C NMR spectra of various hemoglobins in a subsequent paper in this issue (37).

LINEWIDTHS

The experimental linewidth W_{exp} (in hertz) of a single carbon resonance is given by

$$W_{exp} = W_{ins} + W \tag{1}$$

where W_{ins} is the instrumental contribution (from magnetic field inhomogeneity, instabilities, incomplete proton decoupling, digital broadening, and other factors), and W is the natural linewidth. W_{ins} is typically in the range 0.5 to 2 Hz. In studies of small organic molecules, we often have $W < W_{ins}$, so that W_{exp} is dominated by the instrumental contribution. However, in ^{13}C NMR spectra of proteins, the natural linewidth can dominate W_{exp}. Therefore, it is useful to consider the theory of linewidths of ^{13}C resonances.

It has been shown that protonated carbons of large diamagnetic molecules have a natural linewidth overwhelmingly determined by the ^{13}C-^{1}H dipole-dipole relaxation mechanism (35). The effectiveness of this relaxation mechanism is inversely proportional to the sixth power of r_{CH}, the distance between the ^{13}C and ^{1}H nuclei (see below). Fig. 3 indicates that r_{CH}^{-6} is about 60 times greater for directly bonded CH groups ($r_{CH} \approx 1.09$ A) than for the closest nonbonded CH interactions (39, 40). Therefore, ^{13}C-^{1}H dipolar relaxation should be much less effective for nonprotonated carbons than for protonated ones. As a result, one must consider the possibility that relaxation mechanisms other than the ^{13}C-^{1}H dipolar one contribute significantly to the natural linewidths of nonprotonated carbons. The spin-rotation relaxation mechanism (41) can contribute significantly to ^{13}C relaxation in very small molecules, but can be confidently ignored when dealing with large molecules (41, 42). Relaxation arising from chemical shift anisotropy is only important at very high magnetic field strengths (41). One relaxation mechanism that cannot be ignored here is that arising from the dipolar interactions of ^{13}C nuclei with paramagnetic species (1, 3, 4, 43). However, we show in the next section that, in general, the ^{13}C-^{1}H dipolar relaxation mechanism is dominant for nonprotonated aromatic carbons of a native protein (at 14.2 kG).

The contribution to the linewidth of a ^{13}C resonance from the dipolar interactions with all nuclei in the sample is given by Equation 2 (44, 45).

$$W = \sum_j W_j = (15\pi)^{-1} \hbar^2 \gamma_C^2 \sum_j S_j (S_j+1) \gamma_j^2 r_{Cj}^{-6} \phi_j \tag{2}$$

Here γ_C and γ_j are the gyromagnetic ratios of ^{13}C and of nucleus *j*, respectively, S_j is the spin quantum number of nucleus *j*, W_j is the contribution to the ^{13}C linewidth from a dipolar interaction with nucleus *j*, and each ϕ_j is a function of the changes in magnitude and direction of the vector connecting the two nuclei. Because of the dependence of the dipolar interaction on the inverse sixth power of the distance of the ^{13}C nucleus to nucleus *j* (r_{Cj}), only a few terms in Equation 2 are significant. Each ϕ_j in Equation 2 takes a relatively simple form if one assumes that intermolecular dipole-dipole interactions are negligible, that the molecule as a whole rotates isotropically, and that internal motions can be neglected (rigid sphere model). Then (41, 44–46)

$$\phi_j = \chi_j + 4\tau_R + \frac{6\tau_R}{1+\omega_j^2\tau_R^2} \tag{3}$$

where

$$\chi_j = \frac{\tau_R}{1+(\omega_j-\omega_C)^2\tau_R^2} + \frac{3\tau_R}{1+\omega_C^2\tau_R^2} + \frac{6\tau_R}{1+(\omega_j+\omega_C)^2\tau_R^2} \tag{4}$$

Here τ_R is the correlation time for rotational reorientation of the molecule, and ω_C and ω_j are the resonance frequencies, in radians/s, of ^{13}C and of nucleus *j*, respectively.

Within a few per cent accuracy, for a protonated carbon one need only consider the directly bonded hydrogens ($j = {}^{1}H$, $S_H = 1/2$, $r_{CH} = 1.08$ to 1.09 A), and Equation 2 becomes

$$W/\eta = (20\pi)^{-1} \hbar^2 \gamma_C^2 \gamma_H^2 r_{CH}^{-6} \phi_H \tag{5}$$

where η is the number of directly attached hydrogens. In the case of a CH_2 or CH_3 group, we have assumed here that the 2 or 3 hydrogens have the same C—H bond length. When dealing with nonprotonated carbons, each r_{CH} in Equation 2 represents a nonbonded C—H distance. The shortest r_{CH} values, those to hydrogens two bonds removed, are in the range 2.0 to 2.2 A (Fig. 3). Distances of hydrogens to carbons three bonds removed are typically 3 A or longer (39, 40). Because of the relatively large gyromagnetic ratio of ^{1}H, dipolar interactions of nonprotonated carbons with nuclei other than hydrogen generally have been ignored (35, 47, 48). Recently, Moreland and Carroll (49) have pointed out that ^{13}C-^{13}C dipolar relaxation may be important for nonprotonated carbons of ^{13}C-enriched molecules. Even though the natural abundance of ^{14}N is 99.63%, ^{13}C-^{14}N dipolar relaxation has previously been neglected, presumably because the square of the gyromagnetic ratio for ^{14}N is 1/192 of the corresponding value for ^{1}H. However, $S_j(S_j + 1)$ is 0.75 for ^{1}H, but 2 for ^{14}N. More importantly, directly bonded carbon-nitrogen distances are much shorter than nonbonded carbon-hydrogen distances (39, 40). We show in the next section that a nitrogen bonded to a nonprotonated carbon contributes significantly to the relaxation of that carbon.

If the rigid sphere model is applicable, Equation 2 can be used to compute the linewidth of a nonprotonated carbon resonance. For accurate calculations, it is desirable to include not only hydrogens two bonds removed, but also directly bonded nitrogens, and hydrogens three bonds removed, as we do when dealing with T_1 (see "Spin-Lattice Relaxation"). However, as an approximation, we will now consider only the effect of hydrogens two bonds removed. Most of the two-bond CH distances of Fig. 3 are about 2.16 A. Therefore, to a first approximation, Equation 5 can be used, but with $r_{CH} = 2.16$ A, and η defined as the number of hydrogens two bonds removed. A plot of W/η as a function of τ_R is given in Fig. 4 for three commonly used magnetic field strengths.

The use of Equation 5 to compute W requires a knowledge of

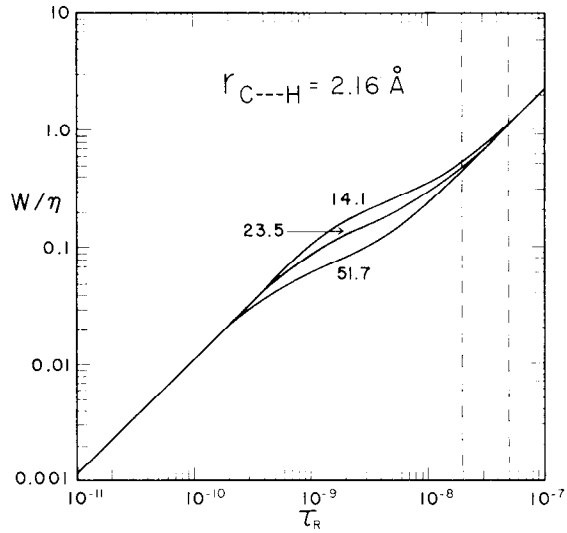

FIG. 4. Log-log plots of W/η (in hertz) *versus* τ_R (in seconds) for a ^{13}C spin relaxing by a dipolar interaction with a single proton 2.16 A away (typical two-bond CH distance), in the case of isotropic rotational reorientation and under conditions of complete proton decoupling. Results are shown for 14.1 kG ($\omega_C = 9.48 \times 10^7$ radians/s, $\omega_H = 3.77 \times 10^8$ radians/s), 23.5 kG ($\omega_C = 1.58 \times 10^8$ radians/s, $\omega_H = 6.29 \times 10^8$ radians/s), and 51.7 kG ($\omega_C = 3.48 \times 10^8$ radians/s, $\omega_H = 1.38 \times 10^9$ radians/s). The *broken vertical lines* are located approximately at the rotational correlation times of the proteins in Table I.

τ_R. We determined the rotational correlation times of horse heart ferrocytochrome *c*, hen egg white lysozyme, horse carbon monoxide myoglobin, and human adult carbon monoxide hemoglobin from T_1 values of C^α, as described previously (10). The resulting τ_R values are presented in Table I. When introduced into Equation 5, these τ_R values yield W/η values of about 30 Hz for protonated carbons of cytochrome *c*, lysozyme, and myoglobin, and about 70 Hz for protonated carbons of hemoglobin. However, there are resonances much narrower than this in the saturated carbon region (Fig. 1) that can only arise from protonated carbons, a clear indication that the rigid sphere model is not applicable to some C—H groups of some aliphatic side chains. We discuss the effects of internal rotation on linewidths in another section of this paper. For nonprotonated aromatic carbons, the predicted value of W/η (Table I) is about 0.5 Hz for cytochrome *c*, lysozyme, and myoglobin, and about 1 Hz for hemoglobin. In the case of C^γ of a tryptophan residue ($\eta = 3$) the calculated linewidth is about 1.5 Hz for cytochrome *c*, lysozyme, and myoglobin, and about 3 Hz for hemoglobin, in agreement with experimental values (see below).

We have computed values of the linewidths that take into account variations in two-bond CH distances (Fig. 3), the effect of directly bonded nitrogens, and the effect of hydrogens more than two bonds removed. However, because of the limited accuracy of our experimental linewidths (±1 Hz), we do not present these refined theoretical linewidths here. Within our experimental accuracy, the observed linewidths are in agreement with the calculated ones. For example, the measured values of W ($W_{exp} - W_{ins}$, where $W_{ins} \approx 1$ Hz) for resolved single carbon resonances of C^γ of tryptophan residues are about 2 Hz and 4 Hz, respectively, in spectra of horse heart ferrocytochrome *c* (Fig. 2*A*) and human adult carbon monoxide hemoglobin (Fig. 2*C*). When going to paramagnetic forms of heme proteins, the resonances of the heme carbons and amino acid carbons that are very near the heme may become significantly broader than in spectra of diamagnetic forms of these proteins (33).

TABLE I

Measured α carbon spin-lattice relaxation times of some proteins, calculated values of W/η and NOE for protonated and nonprotonated carbons, and calculated values of ηT₁ for nonprotonated carbons

Experimental and calculated values are at 14.2 kG. Calculated values assume no internal rotations. For a protonated carbon, η is the number of directly bonded hydrogens (taking r_{CH} = 1.09 A). For a nonprotonated carbon, η is the number of hydrogens two bonds removed (taking r_{CH} = 2.16 A).

	HORSE-HEART CYTOCHROME *C*	HEN EGG-WHITE LYSOZYME	HORSE MYOGLOBIN	HUMAN ADULT HEMOGLOBIN
Molecular weight[a]	12,300	14,300	17,600	64,500
Measured C^α T_1 (ms)[b]	29[c]	31[d]	30[e]	62[f]
τ_R (ns)[g]	17	20	19[h]	47
W/η, protonated (Hz)[i]	30	33	32	67
W/η, nonprotonated (Hz)[j]	0.49	0.55	0.53	1.11
ηT₁, nonprotonated (s)[k]	1.73	1.90	1.84	3.76
NOE[l]	1.21	1.19	1.20	1.16

[a] Rounded off to the nearest 100. Based on polypeptide chain values of Ref. 38, and a residue weight of 616.5 for the heme.

[b] Estimated accuracy is ±15%.

[c] Horse-heart ferrocytochrome *c* (16 mM) in H_2O (0.1 M NaCl/0.05 M phosphate buffer, pH 5.5) at 36°.

[d] pH 3, 42°. Sample conditions are those of Figs. 7 and 8. An α carbon T_1 value of 31 ms was obtained for the protein in H_2O, and a value of 33 ms for the protein in D_2O.

[e] Horse carbon monoxide myoglobin (8.6 mM) in H_2O (0.1 M NaCl/0.05 M phosphate buffer, pH 6.5) at 36°.

[f] Human adult carbon monoxide hemoglobin (3.7 mM) (in tetramer) in H_2O (0.1 M NaCl/0.05 M phosphate buffer, pH 6.9) at 36°.

[g] Computed using the experimental α carbon T_1 values and Equation 7, with $\eta = 1$.

[h] A value of 22 ± 5 ns has been reported for 16 mM sperm whale cyanoferrimyoglobin at 30° and pH 7.5 (11).

[i] Computed value for a protonated carbon, using Equation 5 and the given τ_R value.

[j] Computed value for a nonprotonated carbon, using Equation 5 and the given τ_R value.

[k] Computed value for a nonprotonated carbon, using Equation 7 and the given τ_R value.

[l] Computed using Equation 9.

SPIN-LATTICE RELAXATION

The spin-lattice relaxation times of the nonprotonated carbon resonances in our protein spectra can be measured more accurately than the linewidths. Spin-lattice relaxation times can be used to determine relaxation mechanisms (41) and to measure over-all and internal rotational motions in molecules (10, 35, 41, 50). T_1 values can also be used for assigning ^{13}C resonances (31, 35, 47, 48, 51, 52). Furthermore, a knowledge of T_1 values is useful for choosing instrumental conditions that maximize signal to noise ratios (53).

When Equation 2 is valid for the linewidth, the corresponding rigid sphere expression for spin-lattice relaxation is Equation 6 (41, 44–46).

$$1/T_1 = \sum_j 1/T_{1j} = \frac{2}{15}\hbar^2\gamma_C^2\sum_j S_j(S_j+1)\gamma_j^2 r_{Cj}^{-6}\chi_j \qquad (6)$$

Here $1/T_{1j}$ is the contribution to $1/T_1$ from a dipolar interaction between the pertinent ^{13}C nucleus and nucleus *j*. All other quantities have been defined in the previous section.

If only hydrogens equidistant from the pertinent carbon are considered, we get Equation 7 for $1/\eta T_1$, which is analogous to

Equation 5 for W/η.

$$1/\eta T_1 = \frac{1}{10}\hbar^2\gamma_C{}^2\gamma_H{}^2 r_{CH}{}^{-6}\chi_H \qquad (7)$$

Equation 7 is most applicable to protonated carbons, with η defined as the number of directly bonded hydrogens, but it can also be used as a first approximation for nonprotonated aromatic carbons if we neglect all interactions except those with hydrogens two bonds removed. A plot of the resulting ηT_1 as a function of τ_R is given in Fig. 5 for three commonly used magnetic field strenghts. Introduction of r_{CH} = 2.16 A and the τ_R values of Table I into Equation 7 yields ηT_1 values for nonprotonated carbons of the proteins under consideration. Theoretical values for a magnetic field strength of 14.2 kG are given in Table I.

The ηT_1 values for nonprotonated carbons given in Table I do not take into account variations in two-bond C—H distances (Fig. 3), and they neglect dipolar interactions with directly bonded nitrogens and with hydrogens more than two bonds removed. Table II gives the more rigorous T_1 values calculated from Equation 6, with the summation carried out over all hydrogens that are two and three bonds removed, and directly bonded nitrogens. If H_2O is the solvent, the resonances of $C^{\delta 2}$ of tryptophan residues have longer calculated T_1 values than all other nonprotonated aromatic carbons, including $C^{\epsilon 2}$ of tryptophan residues. If the hydrogen on $N^{\epsilon 1}$ of a tryptophan residue is replaced by deuterium, than the calculated T_1 value of $C^{\epsilon 2}$ increases by about a factor of 1.6 and becomes comparable to the T_1 of $C^{\delta 2}$ (Table II). The gyromagnetic ratio of ^2H is smaller by a factor of about 6.5 than that of ^1H. It follows from Equation 6 that ^2H-^{13}C dipolar relaxation is negligible in relation to ^1H-^{13}C relaxation, for comparable carbon-deuterium and carbon-hydrogen distances. Note that ^2H and ^{14}N both have S_j = 1, and that the gyromagnetic ratio of ^{14}N is about one-half that of ^2H. Nevertheless, because of the short CN bond length (relative to nonbonded CH distances), ^{13}C-^{14}N dipolar relaxation can contribute significantly to $1/T_1$ of a nonprotonated carbon which has a directly attached nitrogen, especially if $\tau_R \gtrsim$ 10 ns (Fig. 6). Calculated T_1 values that do not include the effect of directly bonded ^{13}C-^{14}N dipolar interactions are shown in parentheses in Table II. The relative contribution to $1/T_1$ from ^{13}C-^{14}N dipolar relaxation increases as the competition from dipolar relaxation by hydrogens two bonds removed decreases (Table II). We calculate a nitrogen contribution of about 40% to $1/T_1$ of $C^{\epsilon 2}$ of tryptophan residues of proteins in D_2O (Table II). In the case of C^{ζ} of arginine residues, the calculated contribution from ^{13}C-^{14}N dipolar relaxation dominates $1/T_1$ when D_2O is the solvent (Table II).

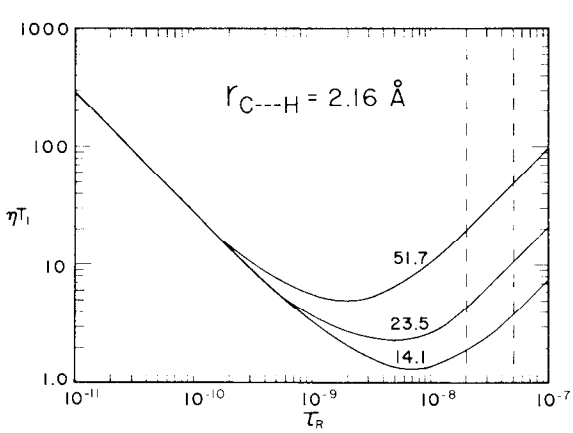

FIG. 5. Log-log plots of ηT_1 *versus* τ_R (both in seconds), for three commonly used magnetic field strengths (in kiloGauss). See caption of Fig. 4 for other details.

We have measured the T_1 values of resolved nonprotonated aromatic carbon resonances and C^{ζ} of arginine residues of horse heart cyanoferricytochrome *c* and hen egg white lysozyme. Measurement of the intensities of narrow resonances that overlap with broad bands of methine-carbon resonances is facilitated if the broad bands are removed by means of the convolution-difference method (54). Details are given in the following paper (33).

The regions of aromatic carbons and C^{ζ} of arginine residues in convolution-difference PRFT ^{13}C NMR spectra of hen egg white lysozyme in H_2O and D_2O are shown in Figs. 7 and 8, respectively. The corresponding NFT spectrum is also shown

TABLE II

Calculated and experimental T_1 values of nonprotonated aromatic carbons and C^{ζ} of arginine residues of native proteins at 14.2 kG

All T_1 values are in seconds. Theoretical values were calculated from Equation 6, using the τ_R values of Table I. Dipolar interactions with ^1H nuclei two and three bonds removed were considered, as well as directly bonded ^{13}C-^{14}N dipolar interactions. Calculated T_1 values that omit the effect of directly bonded nitrogens are given in parentheses. Calculated T_1 values for proteins in D_2O were obtained under the assumption that all O—H hydrogens of tyrosine residues and all side chain N—H hydrogens of histidine, tryptophan, and arginine residues are replaced by deuterium. Experimental T_1 values of hen egg white lysozyme were obtained from the spectra of Figs. 7 to 9. Experimental T_1 values of horse heart cyanoferricytochrome *c* in H_2O were obtained from Fig. 9, *A* and *B* of the following paper (33), and a PRFT spectrum with τ = 0.25 s. Experimental values for cyanoferricytochrome *c* in D_2O were obtained from the PRFT spectrum of Fig. 9*C* in the following paper (33), and an NFT spectrum of the same sample. Estimated accuracy of experimental values is ±25%. Assignments are taken from Ref. 33.

CARBON [a]	CYTOCHROME *C*		LYSOZYME		HEMOGLOBIN
	CALCULATED	EXP. [b]	CALCULATED	EXP. [b]	CALCULATED
Tyr C^{ζ} (H_2O)	0.45	0.4	0.49	0.5	0.97
Tyr C^{ζ} (D_2O)	0.79	0.4	0.87	0.6	1.72
Phe C^{γ}	0.40	0.3	0.44	—	0.86
Trp $C^{\epsilon 2}$ (H_2O)	0.57 (0.73)	0.4	0.62 (0.80)	0.5	1.22 (1.59)
Trp $C^{\epsilon 2}$ (D_2O)	0.94 (1.50)	0.7	1.03 (1.65)	0.7	2.02 (3.27)
His C^{γ} (H_2O) [c]	0.36 (0.40)	0.4	0.39 (0.44)	0.3	0.77 (0.86)
His C^{γ} (H_2O) [d]	0.45 (0.52)	—	0.49 (0.57)	—	0.98 (1.13)
His C^{γ} (D_2O) [e]	0.46 (0.53)	—	0.51 (0.59)	0.4 [c]	1.00 (1.16)
Tyr C^{γ}	0.40	0.4	0.44	0.4	0.86
Trp $C^{\delta 2}$	1.09	0.7	1.20	0.8 [f]	2.36
Trp C^{γ}	0.51	0.4	0.56	0.5 [g]	1.11
Arg C^{ζ} (H_2O)	0.21 (0.27)	0.2	0.23 (0.29)	0.4–0.7 [h]	0.46 (0.58)
Arg C^{ζ} (D_2O)	0.87 (~5)	0.4	0.94 (~6)	0.9–1.5 [i]	1.84 (~11)

[a] Solvents are given in parentheses for carbons that have theoretical T_1 values that change significantly when going from H_2O to D_2O.

[b] Experimental value.

[c] Histidine residue in the imidazolium form.

[d] Histidine residue in the imidazole form.

[e] Histidine residue in the imidazolium or imidazole form.

[f] Based on Peaks 16, 18, 19, and 21 of Figs. 7 and 8, which have been assigned to $C^{\delta 2}$ of 4 of the 6 tryptophan residues (33). Peak 20, which has been assigned to $C^{\delta 2}$ of the other 2 tryptophan residues (33), exhibits a longer T_1 for at least one of its components (Figs. 7 and 8).

[g] The C^{γ} resonance of 1 tryptophan residue (Peak 25 of Figs. 7 and 8) has a slightly longer T_1 value than the other resonances of C^{γ} of tryptophan residues (Peaks 22 to 24 and 26 of Figs. 7 and 8). The difference is small but reproducible. A possible interpretation is given in the following paper in this issue (33).

[h] T_1 values are given in Fig. 9*A*.

[i] T_1 values are given in Fig. 9*B*.

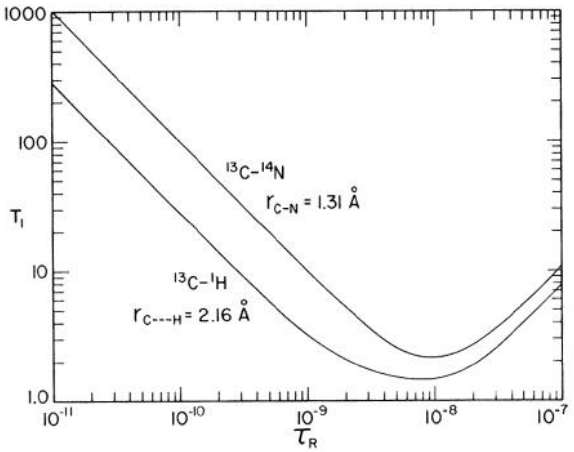

FIG. 6. Comparison of the ^{13}C T_1 value resulting from a dipolar interaction with 1 hydrogen 2.16 A away (typical two-bond CH distance) and the ^{13}C T_1 value resulting from a dipolar interaction with 1 nitrogen 1.31 A away (typical aromatic C—N bond length). T_1 and τ_R are both in seconds. The magnetic field strength was 14.2 kG. Equation 6 was used.

in each case. We define an NFT spectrum as one obtained with the use of 90° radiofrequency pulse excitation (53, 55), and with the interval between successive 90° pulses sufficiently long (relative to the pertinent T_1 values) to ensure that the peak intensities do not differ measurably from the equilibrium intensities (53, 55). The spectra of Figs. 7 and 8 were recorded under conditions of noise-modulated off-resonance proton decoupling (27, 36). This decoupling procedure facilitates the identification of those resonances of nonprotonated aromatic carbons that overlap with broad methine carbon bands (27, 33). Peaks 4 to 26 (NFT spectra of Figs. 7 and 8) arise from the 28 nonprotonated aromatic carbons (33). The resonances of C^{ζ} of the 11 arginine residues (truncated in Figs. 7 and 8) are shown in Fig. 9, but without application of the convolution-difference procedure. The spectra of Figs. 7 to 9, together with one

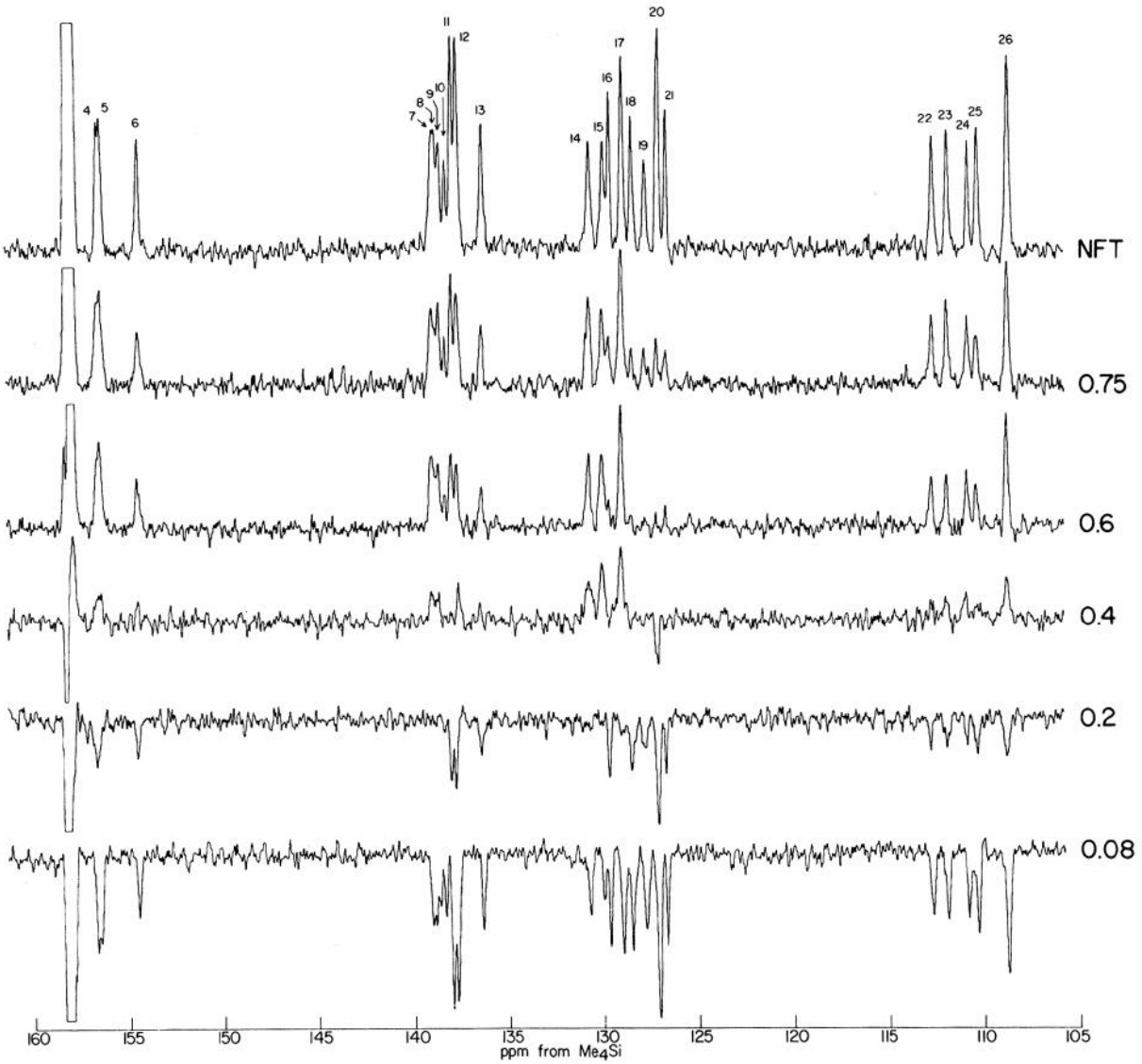

FIG. 7. Region of aromatic carbons and C^{ζ} of arginine residues in convolution-difference natural abundance ^{13}C NFT and PRFT NMR spectra of 14.6 mM hen egg white lysozyme in H_2O (0.1 M NaCl, pH 3.1) at 44°. Each spectrum was recorded at 15.18 MHz, under conditions of noise-modulated off-resonance proton decoupling, using 8,192 time domain addresses, a spectral width of 3,787.9 Hz, and 49,152 accumulations. The convolution-difference procedure was carried out as in Fig. 11 of the following paper (33). Peak numbers in the NFT (*top*) spectrum are those of Table III and Ref. 33. Chemical shifts are given in Table I of Ref. 33. The NFT spectrum was recorded using a recycle time of 2.205 s. The *large number* to the *right* of each PRFT spectrum is τ, in seconds. Each PRFT spectrum was recorded using a recycle time of τ + 2.205 s. The resonances of C^{ζ} of arginine residues (peaks 1 to 3) are fully shown in Fig. 9*A*, but without application of the convolution-difference method.

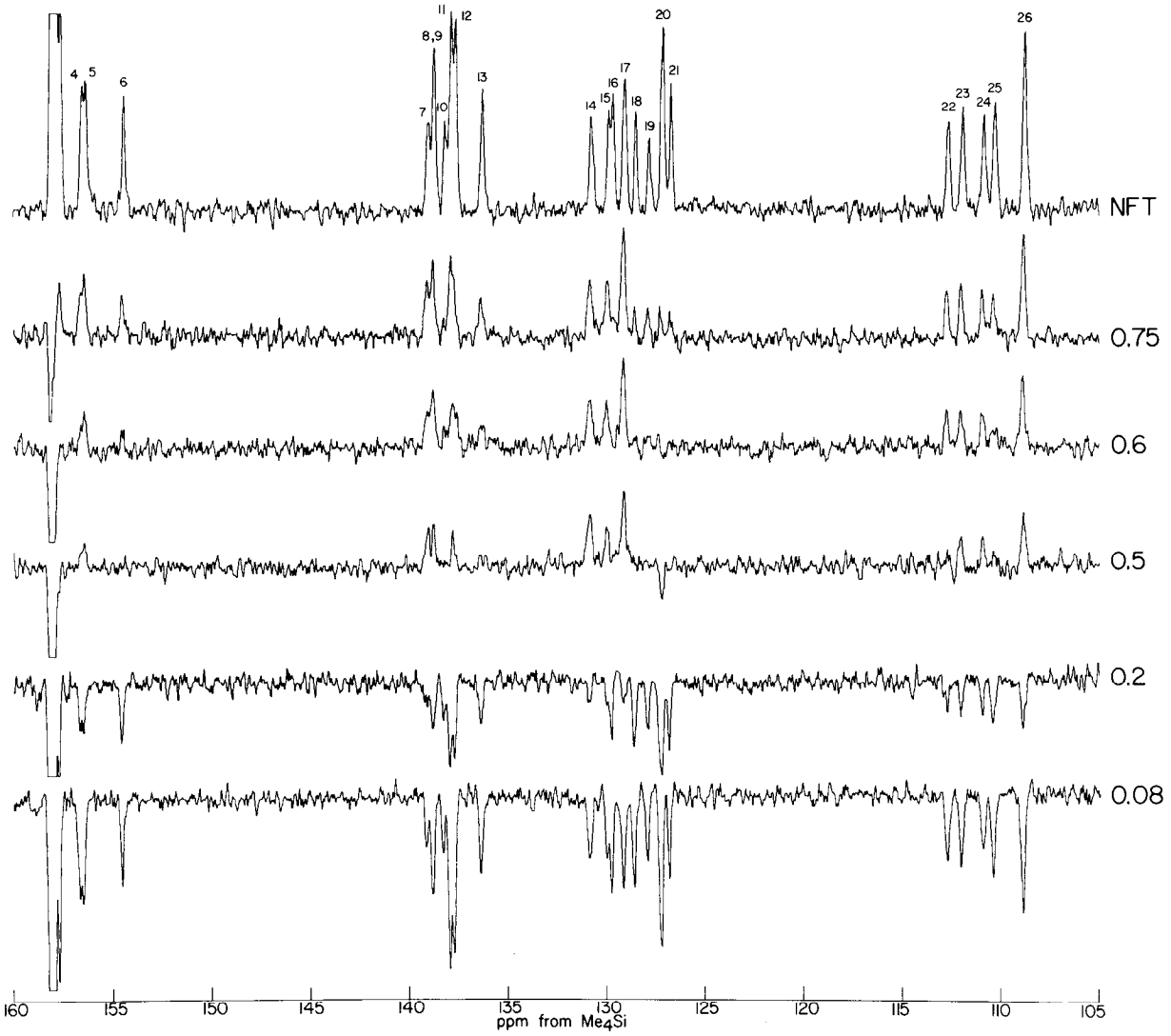

FIG. 8. Region of aromatic carbons and C^{ζ} of arginine residues in convolution-difference natural abundance ^{13}C NFT and PRFT NMR spectra of 13.8 mM hen egg white lysozyme in D_2O (0.1 M NaCl, pH meter reading 3.1) at 42°. Each spectrum was recorded at 15.18 MHz, using the same accumulation and processing conditions as in Fig. 7. Peak numbers in the NFT (*top*) spectrum are those of Table III and Ref. 33. Chemical shifts are given in Table I of Ref. 33. The *large number* to the *right* of each PRFT spectrum is τ, in seconds. The resonances of C^{ζ} of arginine residues (Peaks 1 to 3) are fully shown in Fig. 9*B*, but without application of the convolution-difference method.

additional NFT spectrum in each case, yielded the experimental T_1 values of lysozyme given in Table II.

NFT and PRFT spectra of the paramagnetic horse heart cyanoferricytochrome *c* were also recorded. The resulting T_1 values are given in Table II. The nonprotonated aromatic carbons of the heme were not identified in this case (33). The resonance of C^{γ} of the coordinated His-18 was detected (33), but it was not included in Table II.

We defer the discussion of the T_1 values of C^{ζ} of arginine residues to the section under "Effects of Internal Rotation." Most experimental T_1 values of nonprotonated aromatic carbons are in reasonable agreement with the theoretical ones (Table II). On the whole, the assumptions of rigid rotor behavior and predominantly ^{13}C-^{1}H (and ^{13}C-^{14}N) dipolar relaxation appear to be valid. Note that in the case of cyanoferricytochrome *c*, the results of Table II may not apply to carbons near the paramagnetic center.

NUCLEAR OVERHAUSER ENHANCEMENT

Carbon 13 NMR spectra are normally recorded under conditions of proton decoupling. When ^{13}C relaxation occurs by means of dipolar interactions with ^{1}H nuclei, an important consequence of proton decoupling is an increase in the intensity of the ^{13}C resonances, called the nuclear Overhauser enhancement (41, 56). Here we define the NOE as the ratio of the integrated intensity of a ^{13}C resonance under conditions of proton decoupling and the integrated intensity of the same resonance when no proton decoupling is applied. Because different ^{13}C resonances may have different NOE values, a knowledge of the NOE is essential if one wishes to use integrated intensities to determine the number of carbons that contributes to each resonance. Grant and co-workers (41, 56) have shown that if the relaxation mechanism is purely ^{13}C-^{1}H dipolar and if molecular motion is sufficiently fast to satisfy the extreme narrowing condition (Equation 8), then the NOE has a value of 2.988.

$$(\omega_H + \omega_C)\tau_R << 1 \qquad (8)$$

When Equation 8 is not satisfied, and/or if relaxation mechanisms other than the ^{13}C-^{1}H dipolar one contribute significantly, then the NOE will be smaller than the maximum value of 2.988 (41).

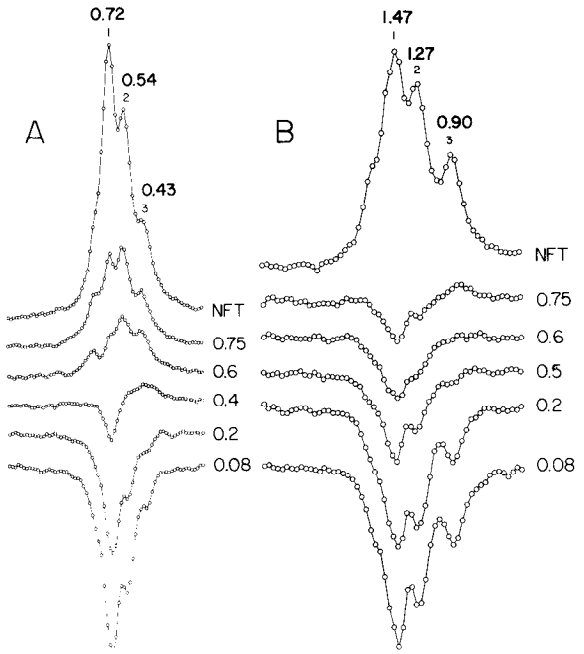

FIG. 9. Resonances of C^{ζ} of arginine residues in NFT and PRFT NMR spectra of hen egg white lysozyme in H_2O (*A*) and D_2O (*B*). *Small numbers above* the peaks of the NFT (*top*) spectra are the peak designations used in Table III and Ref. 33. Chemical shifts are given in Table I of Ref. 33. The *large numbers above* the peaks of the NFT spectra are T_1 values, in seconds. The *large number* to the *right* of each PRFT spectrum is τ, in seconds. *A* and *B* were obtained from the same time domain data as the spectra of Figs. 7 and 8, respectively. The convolution-difference procedure was not applied. A digital broadening of 0.44 Hz was used. The *circles* are the digital points, spaced 0.462 Hz apart.

When the relaxation mechanism is purely ^{13}C-^{1}H dipolar, the rigid sphere expression for the NOE is Equation 9 (41, 46).

$$\mathrm{NOE} = 1 + \frac{\gamma_H}{\gamma_C \chi_H}\left[\frac{6\tau_R}{1+(\omega_H+\omega_C)^2\tau_R^2} - \frac{\tau_R}{1+(\omega_H-\omega_C)^2\tau_R^2}\right] \qquad (9)$$

All of the terms on the right-hand side of Equation 9 have been defined in the section under "Linewidths." Note that CH distances are not present here. The rigid sphere model and a relaxation mechanism totally dominated by ^{13}C-^{1}H dipolar interactions are the only requirements for the validity of this expression. Fig. 10 shows a plot of the NOE *versus* τ_R, calculated from Equation 9, for three commonly used magnetic field strengths. Application of Equation 9 to our proteins yields the calculated NOE values of Table I. In the limit of very slow rotation, given by $(\omega_H + \omega_C)\ \tau_R \gg 1$, Equation 9 predicts the minimum NOE (for ^{13}C-^{1}H dipolar relaxation) of 1.153 (46). The calculated NOE values for proteins (Table I) are close to this minimum value.

We have measured the NOE of some resolved single carbon resonances of horse carbon monoxide myoglobin and horse heart ferrocytochrome *c*. The direct determination of the NOE requires a measurement of the integrated intensities in ^{13}C NMR spectra recorded with and without proton decoupling. Unfortunately, the nonprotonated aromatic carbons yield broad resonances in the absence of proton decoupling, as a result of unresolved splittings from long range ^{13}C-^{1}H scalar coupling. Because of the expected short T_1 values of ^{1}H resonances of proteins, we have not attempted the use of gated proton decoupling (57) for accurate ^{13}C NOE measurements.

In the case of carbon monoxide myoglobin, we first measured the NOE of the ^{13}C resonance of bound carbon monoxide 28.5% enriched in ^{13}C. The NOE measurement is easy in this case because the ^{13}C nucleus of the CO ligand does not show appreciable scalar coupling to any protons. If the NOE of the ^{13}C resonance of the ligand is known, a comparison of the integrated intensity of this resonance in the proton-decoupled spectrum with the integrated intensity of another single carbon resonance yields the NOE of the latter. Integrated intensities of the ^{13}C resonance of the carbon monoxide ligand, recorded with and without proton decoupling yielded an NOE of 1.2 ± 0.1. The integrated intensity of the carbon monoxide resonance in a proton-decoupled spectrum was compared with the integrated intensities of the C^{γ} resonances of the 2 tryptophan residues in the same spectrum. This comparison yielded an NOE of 1.4 ± 0.2 for the tryptophan resonances, within experimental error of the theoretical value in Table I.

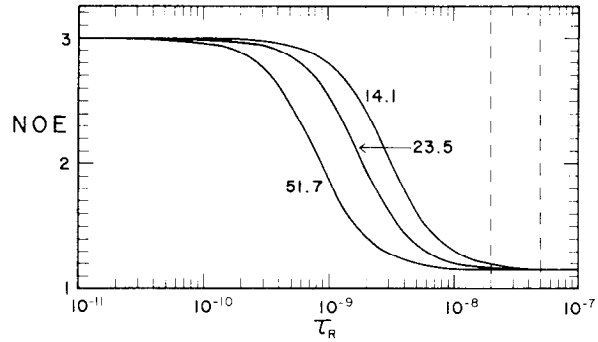

FIG. 10. Semi-log plots of NOE *versus* τ_R (in seconds) for a ^{13}C spin undergoing purely ^{13}C-^{1}H dipolar relaxation, calculated from Equation 9. Results are shown for three commonly used magnetic field strengths (in kiloGauss). The *broken vertical lines* are located approximately at the τ_R values of the proteins in Table I.

In a second type of NOE determination, we used a known concentration of an unbound small molecule that has ^{13}C resonances with known NOE values. We chose sucrose as a suitable standard. The ^{13}C resonances of aqueous sucrose have the full NOE of 3 (35). The relaxation times of the 11 protonated carbons of aqueous sucrose are $\lesssim$0.7 s at 42° (35). Reported chemical shifts of sucrose (58) indicate that 7 of the 11 protonated carbon resonances will generally not overlap with any protein signals. Five of these seven resonances are fully resolved. Finally, sucrose is not expected to bind appreciably to many proteins of interest. Hen egg white lysozyme is one possible exception (59). Irrotational binding to a protein could lower the NOE of sucrose resonances (35, 46). However, such binding would also produce a severe and easily detectable broadening of the protonated carbon resonances of sucrose. Furthermore, if we find a protein carbon resonance with an NOE about one-third that of the sucrose resonances, then the sucrose NOE must be about 3, because 2.988 is the absolute upper limit for the NOE of a ^{13}C resonance. We used the sucrose method to determine the NOE of some resonances in the spectrum of horse heart ferrocytochrome *c* (Fig. 11). The resulting NOE values (Fig. 11) are within experimental error of the theoretical value of 1.2 for this protein (Table I).

We have not measured the NOE of the nonprotonated aromatic carbon resonances of hen egg white lysozyme. However, we have measured the integrated intensities of these resonances and those of C^{ζ} of arginine residues in noise-modulated off-resonance proton-decoupled ^{13}C NMR spectra of lysozyme in H_2O and in D_2O (Table III). Within the accuracy (±20%) of our integrals, the resonances of the 28 nonprotonated aromatic carbons of lysozyme in H_2O (*Peaks 4*

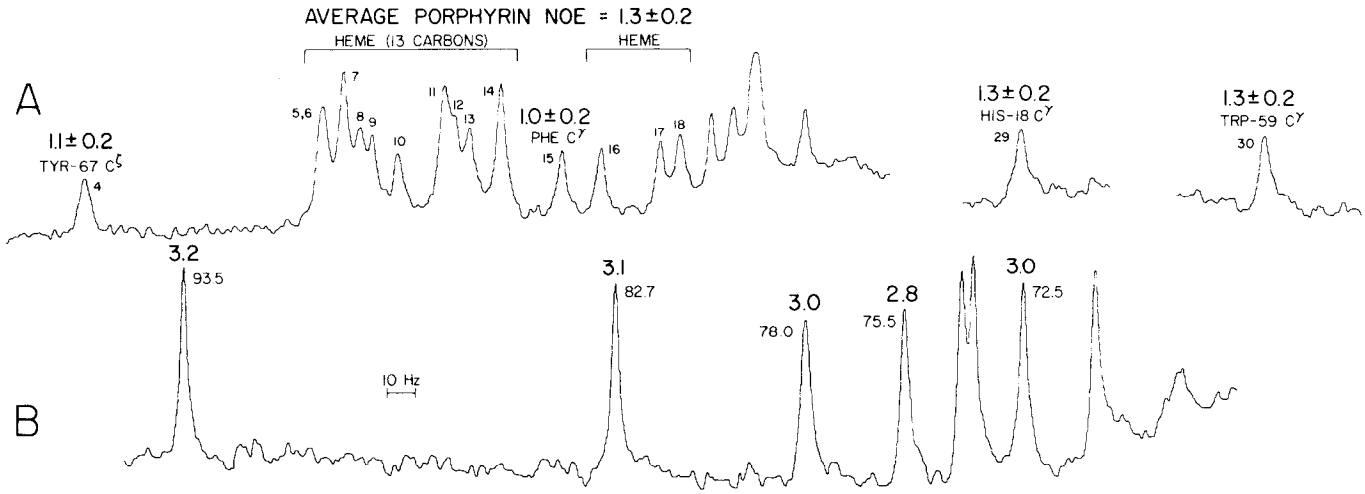

FIG. 11. Fully proton-decoupled natural abundance ^{13}C Fourier transform NMR spectrum (at 15.18 MHz) of 10 mM sucrose and 12.5 mM horse heart ferrocytochrome *c* in H_2O (0.1 M NaCl/0.05 M phosphate buffer, pH 6.8) at 39°, after 30,012 accumulations with a recycle time of 2.105 s (17.5 hours total time), 16,384 time domain addresses and a spectral width of 4,000 Hz. *A*, some resonances of nonprotonated aromatic carbons of the protein. *Small numbers* are peak designations of Fig. 2*A* and Ref. 33. Chemical shifts and assignments are given in Ref. 33. *Large numbers* are NOE values obtained from a comparison of the integrated intensities of these resonances with those of five well resolved sucrose resonances. *B*, methine-carbon resonances of sucrose. The vertical scale is 1.25 times that of the protein resonances in *A*, to compensate for the lower sucrose molarity. The *small numbers* are chemical shifts (in parts per million downfield from Me_4Si) of the five well resolved resonances having integrated intensities that were used to determine the NOE of the protein carbons. *Large numbers* are integrated intensities, normalized to an average of 3.0, the known NOE of these resonances (35).

TABLE III

Integrated intensities of ^{13}C resonances of nonprotonated aromatic carbons and C^{ζ} of arginine residues of hen egg white lysozyme in H_2O and D_2O

Peak numbers are those of Figs. 7 to 9. The sample conditions for the protein in H_2O and in D_2O are given in the captions to Figs. 7 and 8, respectively. Each spectrum was recorded using 98,304 accumulations and a recycle time of 2.205 s (60 hours per spectrum). The convolution-difference method was applied with τ_1 = 0.72 s, τ_2 = 0.036 s, and K = 0.9. τ_1, τ_2, and K are defined in Refs. 33 and 54. Other spectral conditions were the same as for the NFT spectra in Figs. 7 and 8. The recycle time was sufficiently long (relative to the experimental T_1 values of Table II) to get equilibrium intensities, except for the C_{ζ} resonances of arginine residues (Peaks 1 to 3) of the protein in D_2O. The arithmetic average of the intensities of the 28 nonprotonated aromatic carbons was set to unity in each case.

PEAK	NUMBER OF CARBONS[a]	INTENSITY		PEAK	NUMBER OF CARBONS[a]	INTENSITY	
		H_2O	D_2O			H_2O	D_2O
1-3	11	16.6	10.1[b]	17	2	1.7	1.7
4,5	2	2.3	2.3	18	1	0.9	1.0
6	1	1.0	1.0	19	1	1.0	0.9
7-9	3	2.5	2.8	20	2	2.1	2.0
10	1	0.8	0.9	21	1	1.0	1.0
11	2	1.7	2.1	22	1	1.1	1.1
12	2	2.0	1.7	23	1	1.2	1.2
13	1	1.1	1.2	24	1	1.1	1.1
14	1	1.2	0.9	25	1	1.3	1.2
15	1	1.1	2.0	26	2	2.0	2.0
16	1	1.1					

[a] See text.

[b] Some of the resonances contained in this poorly resolved group of peaks have less than equilibrium intensities, because their T_1 values are not much shorter than the recycle time of 2.205 s (Fig. 9*B*).

to *26* in the *top spectrum* of Fig. 7) fall into two categories: Peaks 4 to 10, 13 to 16, 18, 19, 21, and 22 to 25 (a total of 18 resonances) all have the same intensities. Each of the remaining resonances (Peaks 11, 12, 17, 20, and 26) has about twice the intensity of each peak in the first group. However, we do not have to invoke these integrated intensities to conclude that each one of the five peaks in the second group is a 2-carbon resonance, because we have independent evidence for this. The Co^{2+} ion binds in the vicinity of Glu-35 and Asp-52 of lysozyme, and acts as a paramagnetic shift reagent (60). Peaks 17, 20, and 26 each split into two components of equal intensity when Co^{2+} ions are added to the aqueous protein sample.[2] The effect of binding of *N*-(1-oxyl-2,2,6,6-tetramethyl-4-piperidinyl) acetamide (61, 62), a paramagnetic broadening reagent, provides evidence that Peaks 11 and 12 are also 2-carbon resonances.[2] Therefore, Peaks 11, 12, 17, 20, and 26 contain the resonances of a total of 10 carbons. The other 18 peaks must contain the resonances of the remaining 18 carbons, and therefore must be single carbon resonances. We conclude that all of the resonances of nonprotonated aromatic carbons of lysozyme in H_2O have the same intensity (within ±20%). We can reach the same conclusion in the case of lysozyme in D_2O (Table III). Note that Peak 8 undergoes an upfield shift when going from H_2O (Fig. 7) to D_2O solution (Fig. 8). Deuterium isotope effects on ^{13}C chemical shifts of proteins are discussed in the following paper (33).

Because of the long τ_R values of proteins, the calculated NOE for the nonprotonated aromatic carbon resonances is only about 1.2, even if relaxation is purely ^{13}C-^{1}H dipolar. Therefore, a decrease in the NOE as a result of other relaxation mechanisms can be no more than a 20% effect. The limited accuracy of our experimental NOE values prevents the detection of the decrease in NOE of $C^{\epsilon 2}$ of tryptophan residues resulting from a significant ^{13}C-^{14}N dipolar relaxation.

EFFECTS OF INTERNAL ROTATION

The theoretical linewidths, spin-lattice relaxation times, and nuclear Overhauser enhancements presented in the previous sections were computed under the assumption of no internal ro-

[2] R. S. Norton, R. F. Childers, and A. Allerhand, manuscript in preparation.

tation of amino acid side chains. There is some evidence that aromatic residues of native proteins in solution are "immobilized." Browne *et al.* (13) used ^{13}C relaxation measurements on the 4 histidine residues (^{13}C-enriched at $C^{\epsilon 1}$) of the α subunit of tryptophan synthetase to conclude that the histidine residues of the aqueous protein are highly immobilized. Hunkapiller *et al.* (14) reported a similar study of $C^{\epsilon 1}$ of the lone histidine residue of α-lytic protease, and concluded that this residue is held rigidly within the protein. Opella *et al.* (32) reported some ^{13}C relaxation data for the phenylalanine residues of carp parvalbumin which suggest limited internal rotation of the phenylalanine rings. We discuss below the limitations in the use of linewidths, spin-lattice relaxation times, and NOE values for detecting internal rotations of protein side chains.

We have computed the effect of 1 degree of internal rotation on W, T_1, and the NOE of a nonprotonated carbon that is relaxed by one ^1H nucleus 2.17 A away. We have assumed that the molecule as a whole rotates isotropically with a correlation time τ_R and that the C—H vector under consideration undergoes internal rotation with a correlation time τ_G. We chose a value of 105° for the angle (θ) between the C—H vector and the axis of internal rotation. The equations have been presented elsewhere (46). In Fig. 12 we show plots of T_1, W, and the NOE as a function of τ_G, when the correlation time for over-all rotation is 20 ns. The asymptotic values on the right-hand side are the W, T_1, and NOE values in the absence of internal rotation. As internal rotation sets in (going from *right* to *left* in Fig. 12), there are gradual changes in W, T_1, and the NOE. However, if $\tau_G \gtrsim \tau_R$, then the effect of internal rotation on T_1 and the NOE is small. In principle, the linewidth can be used for detecting internal rotation when $\tau_G \lesssim \tau_R$ (Fig. 12). In practice, for nonprotonated carbons of a protein, $W \lesssim W_{ins}$ (see Equation 1) and it is therefore difficult to measure the natural linewidth accurately. However, the natural linewidth of a methine carbon resonance of an immobilized aromatic residue ($\tau_G \gg \tau_R$) is much greater than a typical instrumental broadening (Table I). Therefore, linewidths of resolved methine aromatic carbon resonances may become detectably narrower as a result of internal rotation, when $\tau_G \lesssim$ 10 ns (Fig. 13).

The measured T_1 value of C^ζ of the 2 arginine residues of horse heart cyanoferricytochrome *c* in H_2O (Table II) is consistent with the dominance of the ^{13}C-^1H relaxation mechanism and the lack of detectable segmental motions of the side chain ($\tau_G \gtrsim \tau_R$). The corresponding experimental T_1 value for the protein in D_2O is longer than when H_2O is the solvent, but shorter than the calculated value dominated by ^{13}C-^{14}N dipolar relaxation (Table II). It is possible that not all NH hydrogens of our protein sample (33) were fully exchanged with deuterium. It is also possible that paramagnetic impurities contribute significantly to the relaxation of C^ζ of arginine residues of the protein in D_2O.

In the case of hen egg white lysozyme, segmental motion of some arginine side chains is sufficiently fast to affect T_1 and NOE values of C^ζ. The C^ζ resonances of arginine residues in PRFT spectra of lysozyme in H_2O (Fig. 9*A*) and in D_2O (Fig. 9*B*) indicate that there are considerable variations in the T_1 values of C^ζ of the 11 arginine residues. The longer T_1 values can only arise from C^ζ resonances of arginine side chains undergoing fast segmental motions. This conclusion is supported by the large total integrated intensity (relative to intensities of aromatic carbon resonances) of the resonances of

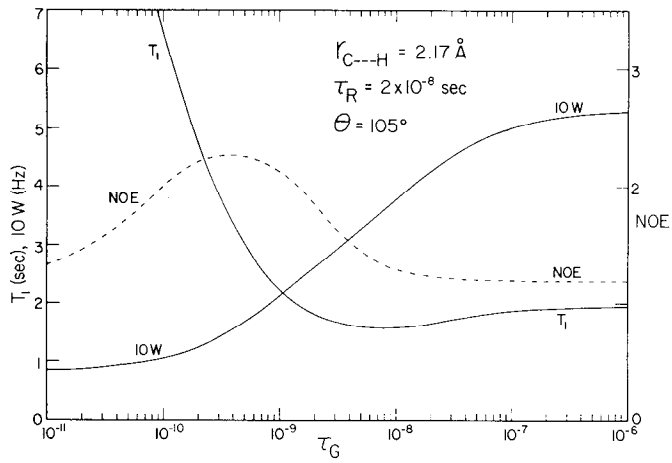

FIG. 12. Semi-log plots of T_1 (in seconds), $W = 1/\pi T_2$ (in hertz), and the NOE as a function of τ_G for a ^{13}C spin relaxing by a dipolar interaction with 1 proton 2.17 A away (typical two-bond CH distance), in the case of isotropic rotation of the molecule as a whole (τ_R = 20 ns), and 1 degree of internal rotation (correlation time τ_G). Equations 37 to 43 of Ref. 46 were used, with a magnetic field strength of 14.2 kG and an angle (θ) between the C—H vector and the axis of internal rotation of 105°.

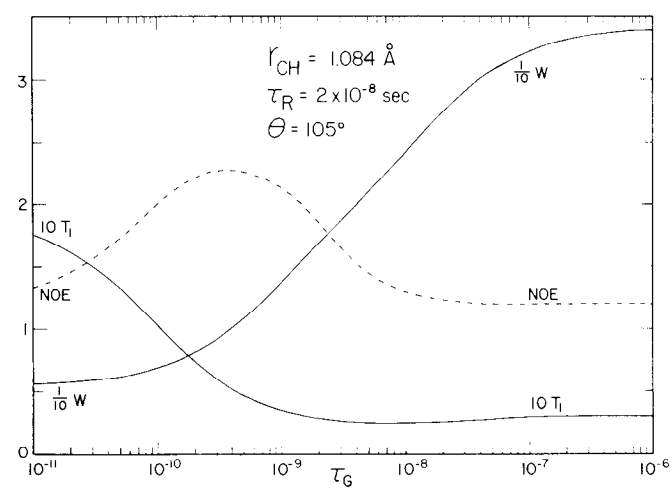

FIG. 13. Same as Fig. 12, but with r_{CH} = 1.084 A (typical C—H bond length).

C^ζ of the 11 arginine residues of the protein in H_2O (Table III). This large intensity indicates a considerable NOE for some (or all) of these 11 resonances. As in the case of horse heart cyanoferricytochrome *c*, the T_1 values of C^ζ of arginine residues of lysozyme in D_2O appear to be about twice as long as the corresponding values when H_2O is the solvent (Fig. 9).

CONCLUSIONS

We have shown that the majority of nonprotonated aromatic carbons of small native proteins (such as cytochrome *c*) yield resolved, narrow, single carbon resonances (Fig. 2*A*). As the size of the protein molecule increases the number of observed single carbon resonances decreases rapidly (at 14.2 kG). For example, natural abundance ^{13}C NMR spectra of hemoglobins yield few resolved individual carbon resonances (Fig. 2*C*). Even though the use of much higher magnetic field strengths than 14.2 kG should greatly increase the number of resolved individual carbon resonances of hemoglobin and other large proteins, high magnetic field strengths may cause some sensitivity problems because of long T_1 values. We have shown that

at 14.2 kG the T_1 values of nonprotonated aromatic carbons of small proteins such as cytochrome *c* and lysozyme are $\lesssim 0.8$ s. Such short T_1 values permit the use of a short recycle time (interval between successive pulses of radiofrequency excitation), so that a large number of spectral scans can be obtained in a reasonable time. We have not measured the T_1 values of nonprotonated aromatic carbons of hemoglobin. At 14.2 kG, T_1 values of about 1 s are expected for most of these carbons (Table II). The calculated values at 51.7 kG are much longer (Fig. 5). For example, the calculated value for C^{γ} of a tyrosine or phenylalanine residue of hemoglobin is about 10 s. Such long T_1 values would greatly reduce the attractiveness of natural abundance ^{13}C Fourier transform NMR for studying single carbon sites of proteins. However, T_1 values at high magnetic field strenghts could turn out to be much shorter than predicted from Fig. 5, if contributions to $1/T_1$ neglected here become large at high fields. Experimental T_1 values at high magnetic field strengths are needed for the purpose of evaluating the feasibility of high frequency ^{13}C NMR studies of proteins.

We have presented experimental T_1 values for some nonprotonated aromatic carbons of horse heart cyanoferricytochrome *c* and hen egg white lysozyme at 14.2 kG. Our results indicate that, in general, the ^{13}C-^{1}H dipolar relaxation mechanism is dominant. However, the relaxation of $C^{\epsilon 2}$ of tryptophan and C^{ζ} of arginine residues has a significant contribution from the ^{13}C-^{14}N dipolar mechanism when D_2O is the solvent. The T_1 values of $C^{\epsilon 2}$ (when $H^{\epsilon 1}$ is replaced by deuterium) and $C^{\delta 2}$ of tryptophan residues are longer than the T_1 values of other classes of nonprotonated aromatic carbons of amino acid residues. This property can be used to identify the resonances of $C^{\delta 2}$ and $C^{\epsilon 2}$ of tryptophan residues by means of the PRFT method (31, 33).

We have presented theoretical and experimental evidence that indicates a uniformly low NOE for the resonances of nonprotonated aromatic carbons of native proteins. Therefore, it is generally safe to make a carbon count on the basis of the integrated intensities of the observed resonances (when the signal to noise ratio is adequate, digital peak definition is sufficient, and the recycle time is long enough). In the following two papers in this issue (33, 37) we present some specific assignments of individual carbon resonances in the natural abundance ^{13}C NMR spectra of some proteins.

Acknowledgments—We thank Professor John M. Hayes for determining the isotopic composition of our ^{13}C-enriched carbon monoxide and Mrs. Carol Williams for her help.

REFERENCES

1. Dwek, R. A. (1973) *Nuclear Magnetic Resonance in Biochemistry*, Oxford University Press, London
2. Roberts, G. C. K., and Jardetzky, O. (1970) in *Advances in Protein Chemistry* (Anfinsen, C. B., Jr., Edsall, J. T., and Richards, F. M., eds) Vol 24, pp. 447–545, Academic Press, New York
3. Wüthrich, K. (1970) *Struct. Bonding* **8,** 53–121
4. Mildvan, A. S., and Cohn, M. (1970) *Adv. Enzymol. Relat. Areas Mol. Biol.* **33,** 1–70
5. Allerhand, A., Cochran, D. W., and Doddrell, D. (1970) *Proc. Natl. Acad. Sci. U. S. A.* **67,** 1093–1096
6. Moon, R. B., and Richards, J. H. (1972) *Proc. Natl. Acad. Sci. U. S. A.* **69,** 2193–2197
7. Nigen, A. M., Keim, P., Marshall, R. C., Glushko, V., Lawson, P. J., and Gurd, F. R. N. (1973) *J. Biol. Chem.* **248,** 3716–3723
8. Bradbury, J. H., and Norton, R. S. (1973) *Biochim. Biophys. Acta* **328,** 10–19
9. Chien, J. C. W., and Wise, W. B. (1973) *Biochemistry* **12,** 3418–3424
10. Allerhand, A., Doddrell, D., Glushko, V., Cochran, D. W., Wenkert, E., Lawson, P. J., and Gurd, F. R. N. (1971) *J. Am. Chem. Soc.* **93,** 544–546
11. Visscher, R. B., and Gurd, F. R. N. (1975) *J. Biol. Chem.* **250,** 2238–2242
12. Packer, E. L., Sternlicht, H., and Rabinowitz, J. C. (1972) *Proc. Natl. Acad. Sci. U. S. A.* **69,** 3278–3282
13. Browne, D. T., Kenyon, G. L., Packer, E. L., Sternlicht, H., and Wilson, D. M. (1973) *J. Am. Chem. Soc.* **95,** 1316–1323
14. Hunkapiller, M. W., Smallcombe, S. H., Whitaker, D. R., and Richards, J. H. (1973) *Biochemistry* **12,** 4732–4743
15. Nigen, A. M., Keim, P., Marshall, R. C., Morrow, J. S., and Gurd, F. R. N. (1972) *J. Biol. Chem.* **247,** 4100–4102
16. Matwiyoff, N. A., Vergamini, P. J., Needham, T. E., Gregg, C. T., Volpe, J. A., and Caughey, W. S. (1973) *J. Am. Chem. Soc.* **95,** 4429–4431
17. Fung, C. H., Mildvan, A. S., Allerhand, A., Komoroski, R., and Scrutton, M. C. (1973) *Biochemistry* **12,** 620–629
18. Nigen, A. M., Keim, P., Marshall, R. C., Morrow, J. S., Vigna, R. A., and Gurd. F. R. N. (1973) *J. Biol. Chem.* **248,** 3724–3732
19. Morrow, J. S., Keim, P., Visscher, R. B., Marshall, R. C., and Gurd, F. R. N. (1973) *Proc. Natl. Acad. Sci. U. S. A.* **70,** 1414–1418
20. Antonini, E., Brunori, M., Conti, F., and Geraci, G. (1973) *FEBS Lett.* **34,** 69–70
21. Koenig, S. H., Brown, R. D., Needham, T. E., and Matwiyoff, N. A. (1973) *Biochem. Biophys. Res. Commun.* **53,** 624–630
22. Brewer, C. F., Sternlicht, H., Marcus, D. M., and Grollman, A. P. (1973) *Biochemistry* **12,** 4448–4457
23. Feeney, J., Burgen, A. S. V., and Grell, E. (1973) *Eur. J. Biochem.* **34,** 107–111
24. Chaiken, I. M. (1974) *J. Biol. Chem.* **249,** 1247–1250
25. Moon, R. B., and Richards, J. H. (1974) *Biochemistry* **13,** 3437–3443
26. Robillard, G., Shaw, E., and Shulman, R. G. (1974) *Proc. Natl. Acad. Sci. U. S. A.* **71,** 2623–2626
27. Allerhand, A., Childers, R. F., and Oldfield, E. (1973) *Biochemistry* **12,** 1335–1341
28. Oldfield, E., and Allerhand, A. (1973) *Proc. Natl. Acad. Sci. U. S. A.* **70,** 3531–3535
29. Allerhand, A., Childers, R. F., and Oldfield, E. (1973) *Ann. N. Y. Acad. Sci.* **222,** 764–777
30. Allerhand, A., Childers, R. F., and Oldfield, E. (1973) *J. Magnetic Res.* **11,** 272–278
31. Oldfield, E., and Allerhand, A. (1975) *J. Am. Chem. Soc.* **97,** 221–224
32. Opella, S. J., Nelson, D. J., and Jardetzky, O. (1974) *J. Am. Chem. Soc.* **96,** 7157–7159
33. Oldfield, E., Norton, R. S., and Allerhand A. (1975) *J. Biol. Chem.* **250,** 6381–6402
34. Vold, R. L., Waugh, J. S., Klein, M. P., and Phelps, D. E. (1968) *J. Chem. Phys.* **48,** 3831–3832
35. Allerhand, A., Doddrell, D., and Komoroski, R. (1971) *J. Chem. Phys.* **55,** 189–198
36. Wenkert, E., Clouse, A. O., Cochran, D. W., and Doddrell, D. (1969) *J. Am. Chem. Soc.* **91,** 6879–6880
37. Oldfield, E., and Allerhand, A. (1975) *J. Biol. Chem.* **250,** 6403–6407
38. Dayhoff, M. O. (ed) (1972) *Atlas of Protein Sequence and Structure* Vol 5, The National Biomedical Research Foundation, Silver Spring, Maryland
39. Tables of Interatomic Distances and Configuration in Molecules and Ions (1965) *Chemical Society of London Special Publication No. 11, Supplement 18* Burlington House, London
40. Wyckoff, R. W. G. (1969) *Crystal Structures* 2nd Ed, Vol 6, Part 1, Interscience, New York
41. Lyerla, J. R., and Grant, D. M. (1972) *Magnetic Resonance, Physical Chemistry Series One* (McDowell, C. A., ed) Vol 4, pp. 155–200, University Park Press, Baltimore
42. Berger, S., Kreissl, F. R., and Roberts, J. D. (1974) *J. Am. Chem. Soc.* **96,** 4348–4349
43. Wasylishen, R. E., and Cohen, J. S. (1974) *Nature* **249,** 847–850
44. Abragam, A. (1961) *The Principles of Nuclear Magnetism* Oxford University Press, London
45. Hertz, H. G. (1967) *Prog. Nucl. Magnetic Res.* **3,** 159–230
46. Doddrell, D., Glushko, V., and Allerhand, A. (1972) *J. Chem.*

Phys. **56,** 3683–3689
47. Wehrli, F. W. (1973) *J. Chem. Soc. Chem. Commun.* 379–380
48. Wehrli, F. W. (1974) *Adv. Mol. Relaxation Processes* **6,** 139–151
49. Moreland, C. G., and Carroll, F. I. (1974) *J. Magnetic Res.* **15,** 596–599
50. Allerhand, A., and Komoroski, R. A. (1973) *J. Am. Chem. Soc.* **95,** 8228–8231
51. Allerhand, A., and Doddrell, D. (1971) *J. Am. Chem. Soc.* **93,** 2777–2779
52. Doddrell, D., and Allerhand, A. (1971) *Proc. Natl. Acad. Sci. U. S. A.* **68,** 1083–1088
53. Ernst, R. R., and Anderson, W. A. (1966) *Rev. Sci. Instrum.* **37,** 93–102
54. Campbell, I. D., Dobson, C. M., Williams, R. J. P., and Xavier, A. V. (1973) *J. Magnetic Res.* **11,** 172–181
55. Farrar, T. C., and Becker, E. D. (1971) *Pulse and Fourier Transform NMR* Academic Press, New York
56. Kuhlmann, K. F., Grant, D. M., and Harris, R. K. (1970) *J. Chem. Phys.* **52,** 3439–3448
57. Freeman, R., Hill, H. D. W., and Kaptein, R. (1972) *J. Magnetic Res.* **7,** 327–329
58. Dorman, D. E., and Roberts, J. D. (1971) *J. Am. Chem. Soc.* **93,** 4463–4472
59. Ikeda, K., and Hamaguchi, K. (1972) *J. Biochem. (Tokyo)* **71,** 265–273
60. McDonald, C. C., and Phillips, W. D. (1969) *Biochem. Biophys. Res. Commun.* **35,** 43–51
61. Berliner, L. J. (1971) *J. Mol. Biol.* **61,** 189–194
62. Wien, R. W., Morrisett, J. D., and McConnell, H. M. (1972) *Biochemistry* **11,** 3707–3716